

SSC-92

LOW TEMPERATURE EMBRITTLEMENT MECHANICS  
DEDUCED FROM ZINC SINGLE CRYSTAL FRACTURE STUDIES

by

Ray Treon, Jr.

and

W. M. Baldwin, Jr.

SHIP STRUCTURE COMMITTEE

# SHIP STRUCTURE COMMITTEE

## MEMBER AGENCIES:

BUREAU OF SHIPS, DEPT. OF NAVY  
MILITARY SEA TRANSPORTATION SERVICE, DEPT. OF NAVY  
UNITED STATES COAST GUARD, TREASURY DEPT.  
MARITIME ADMINISTRATION, DEPT. OF COMMERCE  
AMERICAN BUREAU OF SHIPPING

## ADDRESS CORRESPONDENCE TO:

SECRETARY  
SHIP STRUCTURE COMMITTEE  
U. S. COAST GUARD HEADQUARTERS  
WASHINGTON 25, D. C.

November 10, 1958

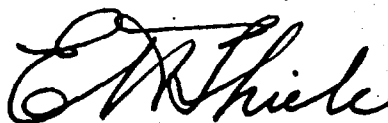
Dear Sir:

The Ship Structure Committee has been concerned with the need to uncover new and fundamental facts about the low temperature embrittlement of metals as an aid toward improving ship steels. As a result, a study has been carried out at Case Institute of Technology. Enclosed herewith is the Final Report, SSC-92, of Project SR-111, entitled "Low Temperature Embrittlement Mechanics Deduced from Zinc Single Crystal Fracture Studies," by Ray Treon, Jr. and W. M. Baldwin, Jr.

This project was conducted under the advisory guidance of the Committee on Ship Steel of the National Academy of Sciences-National Research Council.

This report is being distributed to individuals and groups associated with or interested in the work of the Ship Structure Committee. Please submit any comments that you may have to the Secretary, Ship Structure Committee.

Sincerely yours,



E. H. Thiele, Rear Admiral  
U. S. Coast Guard  
Chairman, Ship Structure Committee

Serial No. SSC-92

Final Report  
of  
Project SR-111

to the

SHIP STRUCTURE COMMITTEE

on

LOW TEMPERATURE EMBRITTLEMENT MECHANICS  
DEDUCED FROM ZINC SINGLE CRYSTAL FRACTURE STUDIES

by

Ray Treon, Jr. and W. M. Baldwin, Jr.

Case Institute of Technology  
Cleveland, Ohio

under

Department of the Navy  
Bureau of Ships Contract NObs-50303  
BuShips Index No. NS-011-078

transmitted through

Committee on Ship Steel  
Division of Engineering and Industrial Research  
National Academy of Sciences-National Research Council

under

Department of the Navy  
Bureau of Ships Contract NObs-72046  
BuShips Index No. NS-731-036

Washington, D. C.  
National Academy of Sciences-National Research Council  
November 10, 1958

## ABSTRACT

This study of the kinematics of fracture of zinc single crystals, made by deforming and examining the crystals in stages, revealed that primary cleavage generally began on the inert side of the kink plane near the shoulder and tended to continue into the shoulder. Increasing the size of the shoulder relative to the area of the actively slipping test section repressed the tendency of the crack to continue into the shoulder. This variation favored further deformation of the test section and thus increased the ductility of the specimens.

This study also confirmed previous work, which showed that orientation gradients, originally wrought by constraints, and not twinning, cause brittle fracture. This is true whether sectional area changes or twinned-untwinned areas change.

## TABLE OF CONTENTS

	<u>Page</u>
I Introduction . . . . .	1
II Materials and Procedure . . . . .	6
III Case Histories . . . . .	7
IV Conclusions . . . . .	27
V References . . . . .	32

## I. INTRODUCTION

Catastrophic failures of such things as gas reservoirs, bridges, Liberty ships, and T-2 tankers have emphasized the need to uncover new and fundamental facts about the low temperature embrittlement of metals. Certain metals become brittle at low temperatures, high strain rates, or hydrostatic tensile stress states. Steels, in the practical sense, are the most important metals in this group, but it was felt that a study of zinc is quite useful, even in the solution of the steel problem, for the following reasons: (1) both zinc and steel become brittle under the test or service conditions mentioned above, both metals twin, and both can fracture by cleavage; and (2) zinc is readily obtained in reasonable purity, it is readily fabricated into single crystals, and its transition temperature from ductile to brittle behavior under the usual testing conditions is conveniently near room temperature.

The first progress report on this project<sup>1</sup> showed that the low temperature brittleness of zinc is not due to a cessation of slip below a certain temperature. On the contrary, slip is quite active, and it is its activity that induces low temperature brittleness. Slip causes rotation of the crystal which in turn sets up orientation gradients, adjacent to constricted and unslipped regions; these orientation gradients are accommodated by bend-planes at high temperatures and by cleavage at low temperatures.

Zinc single crystals generally slip on the basal plane (0001) in the  $[11\bar{2}0]$  direction<sup>2</sup> and twin on the  $(10\bar{1}2)$  plane by shear perpendicular to the  $[\bar{1}2\bar{1}0]$  direction.<sup>3</sup>

As information, the initial orientation angle of the crystal,  $\phi_0$  (Fig. 1a), is the angle between the pole of the basal plane and the tensile axis. The bend-plane (Fig. 1b) is the plane between the two regions of crystal that have slipped by different amounts. Primary slip is slip in the untwinned metal whereas secondary slip occurs in the twinned portion of the crystal. Primary cleavage consists of cleavage on the basal plane of the untwinned material and secondary cleavage takes place on the basal plane of the twinned metal.

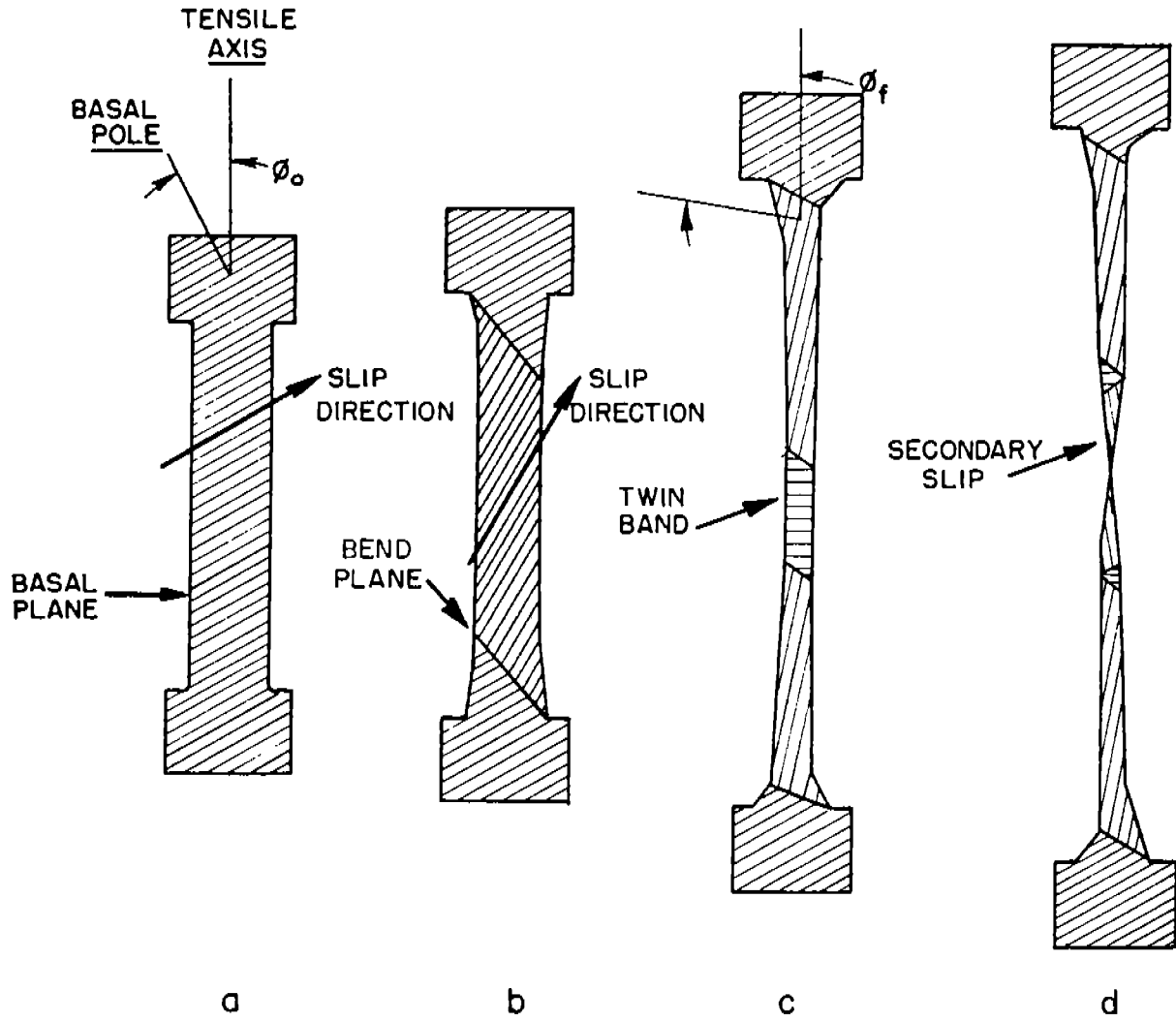


FIG. 1: STEPS IN THE FLOW AND FRACTURE OF A ZINC CRYSTAL.

The previous work under this project produced Fig. 2, which is an idealized representation of ductility (reduction in area) as a function of orientation and temperature for specimens shaped as shown in Figs. 3a and 3c. A description of the specimen surfaces represented in Fig. 2 is summarized as follows:

The Ductile Plateau (Surface A): Specimens having these orientations showed 100 per cent reduction in area at the temperatures shown, although various deformation processes contributed to the final result. Crystals with a starting orientation in the range  $\phi_0 = 0$  to  $80^\circ$  deformed by primary slip to a constant angle  $\phi_f = 80^\circ$ , twinned and then failed by fibrous fracture; crystals with a starting orientation in the range  $\phi_0 = 80$  to  $90^\circ$ , however, twinned with little or no preceding slip before secondary slip led to ductile fracture of the highly necked specimens.

The Brittle Floor Due to Secondary Cleavage (Surface B): At the lower testing temperatures, crystals within an initial orientation range  $\phi_0 = 80$  to  $90^\circ$  twinned and cleaved on the basal plane of the twinned metal.

The Transition Cliff (Surface C): The transition between ductile and brittle behavior of crystals with  $\phi_0 = 80^\circ$  is represented as the cliff (C): this is actually a simplification of the facts, as secondary cleavage can occur statistically at temperatures as high as 75 C, and ductile fractures can occur at temperatures as low as 55 C. The fractures were often of the mixed fibrous and secondary cleavage types in this temperature range.

The Brittle Zone (Surface D): The crystals in this zone deformed by primary slip to a critical terminating orientation,  $\phi_f$ , twinned and then fractured by secondary cleavage. The primary slip that occurred before twinning and cleavage began led to some reduction in area calculable by the equation,

$$\frac{a_0}{a_f} = \frac{\cos \phi_0}{\cos \phi_f} \quad (1)$$

where  $a_0$  and  $a_f$  are the initial and final cross-sectional areas respectively, and  $\phi_0$  and  $\phi_f$  the initial and final orientations. The profile lines ( $d_2$ ) in Zone D were determined in this way.

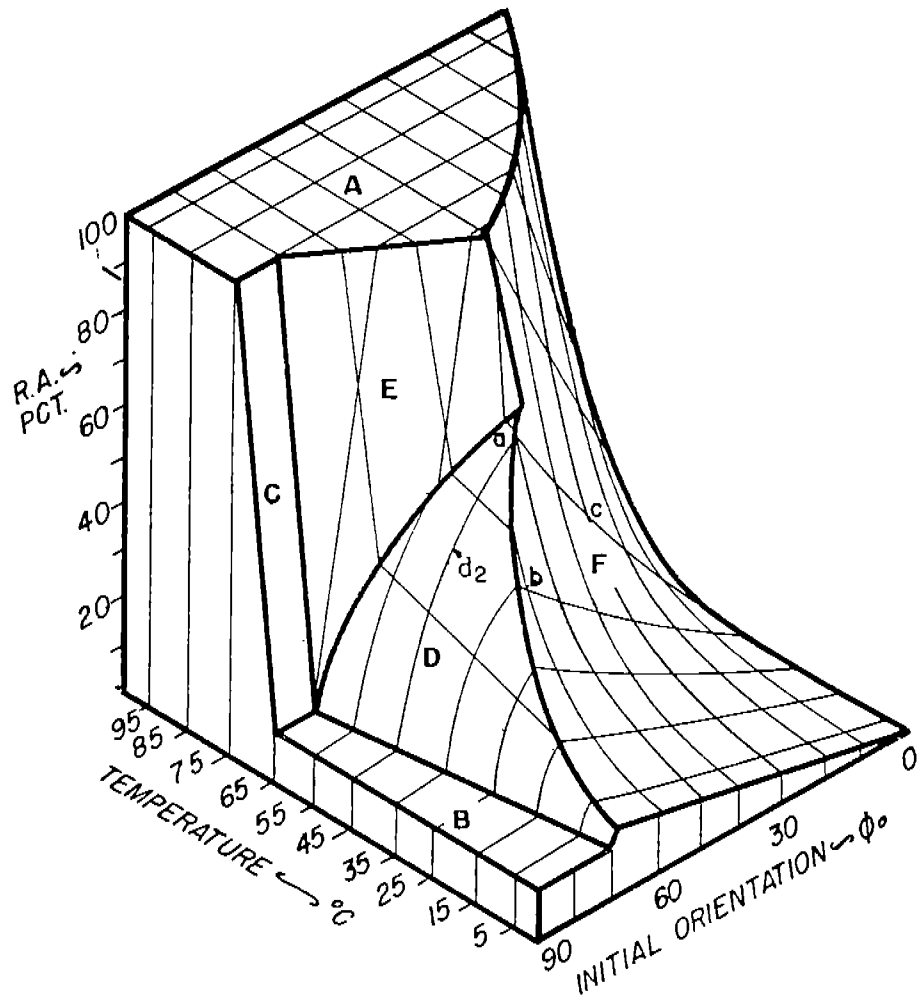


FIG. 2: SIMPLIFIED REPRESENTATION OF DUCTILITY (REDUCTION IN AREA) AS A FUNCTION OF ORIENTATION AND TEMPERATURE FOR 5D SPECIMENS. EACH SURFACE A, B...F, IS DISCUSSED IN DETAIL IN THE TEXT.

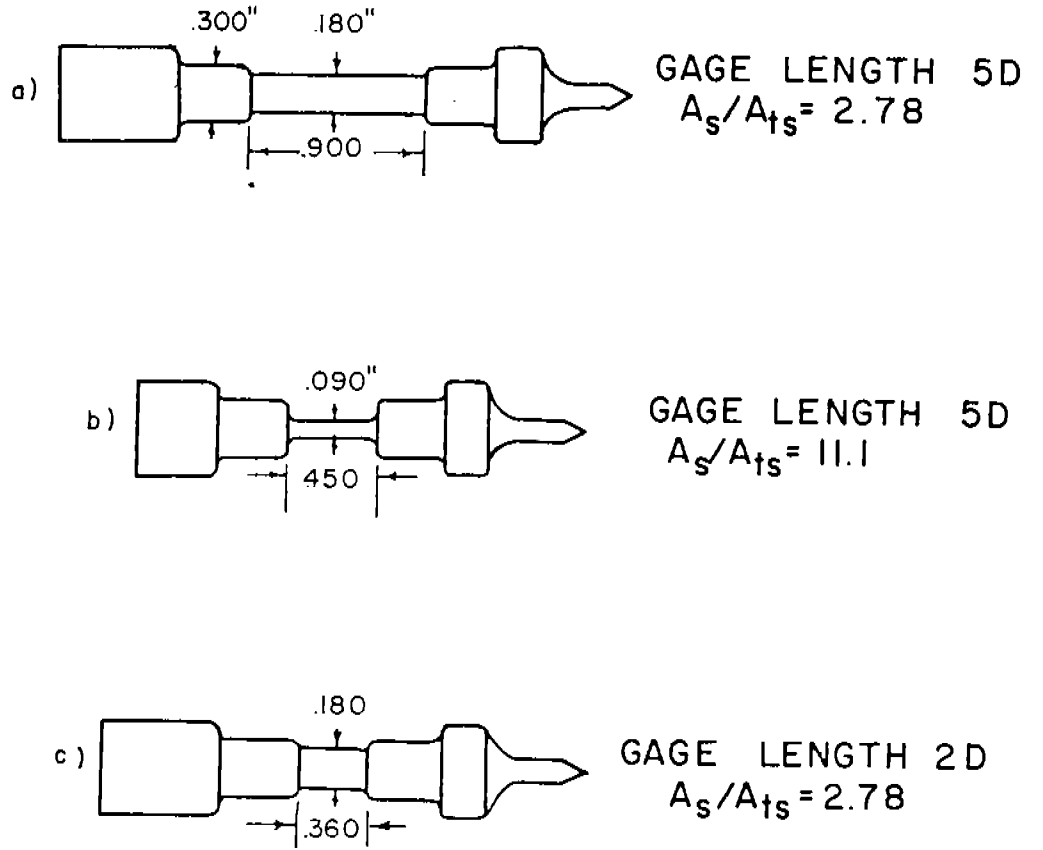


FIG. 3: SHAPE OF SINGLE CRYSTAL SPECIMENS.

The Transition Cliff (Surface E): This range of temperature and orientation is similar to Surface C in that failure of the specimen could be either ductile or brittle, but the range was displaced to lower temperatures as initial orientation decreased. At 55 C, for example, crystals of high initial orientation are brittle, whereas those in the range  $\phi_0 = 40$  to  $60^\circ$  are relatively ductile. Thus a crystal whose orientation was initially greater than  $80^\circ$  would be brittle, while at the same temperature one that rotated by primary slip from a lower value of  $\phi_0$  into the range of  $\phi_0 \geq 80^\circ$  would remain ductile. In this case, primary slip allayed the embrittlement due to secondary cleavage.

The Primary Cleavage Slope (Surface F): In this region, the crystals rotated by primary slip. The orientation gradient at the shoulder was accommodated first by kinking and then by cleavage on the basal plane of the untwinned crystal in the vicinity of the kink.

## II. MATERIALS AND PROCEDURE

In the course of the investigation, a method of growing single crystals of unusual shapes (Fig. 3) from 99.99 per cent pure zinc was developed. A polycrystalline zinc specimen was used as a pattern in an investment mold heated at 1000 F until the zinc melted. The mold was then removed from the furnace and directional cooling was produced by a quenched copper rod acting as a chill. A single crystal nucleated at the contact point of the zinc and copper and grew into the rest of the melt.

To study the kinematics of fracture, a single crystal of zinc was pulled in tension until deformation was visible. It was then carefully removed from the fixture and placed in a microcomparator where its silhouette was traced at a tenfold magnification. Any slip or kink plane lines made visible by a change in the surface of the crystal were also drawn on the shadowgraph of the crystal.

The crystal was placed again in the fixture, deformed further, and a new shadowgraph made. This procedure was repeated until fracture occurred or a desirable stopping point was reached. The crystal was sectioned by cleaving with a razor blade at boiling liquid nitrogen temperature to reveal the basal planes throughout. The silhouette resulting from each such cleavage was drawn on the final shadowgraph. Crystals of the shape of Fig. 3c were employed in this work because an ample supply of these specimens having varying orientations was already available.

### III. CASE HISTORIES

The kinematics of zinc single crystals prior to fracture were studied in detail using forty orientations and temperatures. The orientations and the temperatures at which the specimens were tested are located at points a, b, and c in Fig. 2. This section reports on three specific case histories, describing in detail the behavior of the specimen at each stage of the test. Figures 4--7 represent these stages graphically. From these case histories, it is to be noted that although the behavior of the specimens varied in detail, certain general similarities could be seen.

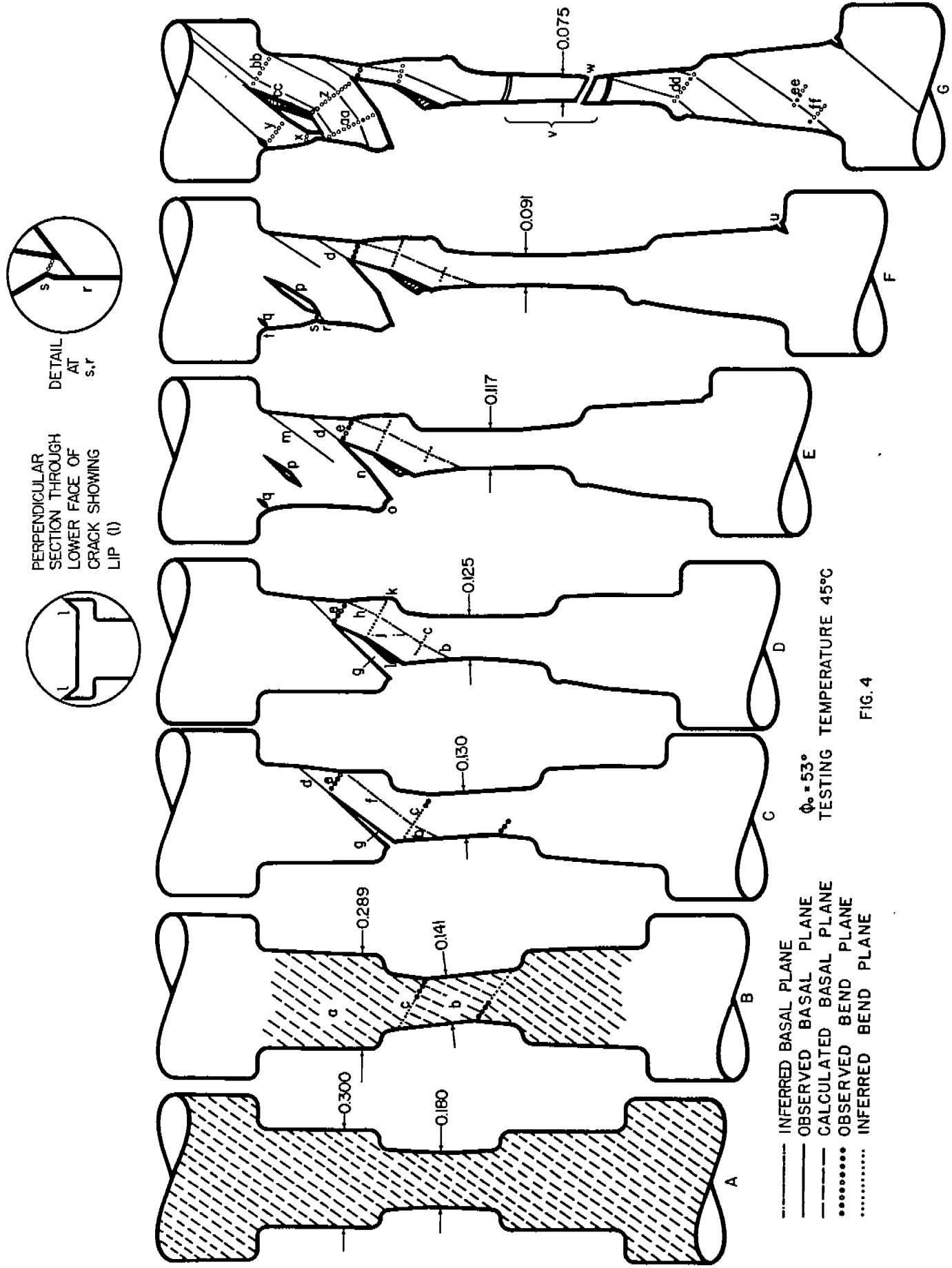
#### Case History I (Fig. 4)

Fig. 4a pictures an undeformed crystal before it was tested at 45 C. The dashed lines represent the basal planes in their original orientation,  $\phi_0 = 53^\circ$ . (This crystal would be plotted on Surface A in Fig. 2.)

The second stage of the test (Fig. 4b) was begun using Eq. (1)

$$\frac{a_0}{a_f} = \frac{\cos \phi_0}{\cos \phi_f}$$

where  $a_0$  is the original cross sectional area and  $a_f$  is the cross sectional area when primary slip ceases. The slip lines (a) were calculated from the original orientation and the reduction in diameter of the shoulder (0.300 to 0.289 in.). In a similar manner, slip lines (b) were calculated for the test section which was reduced in diameter



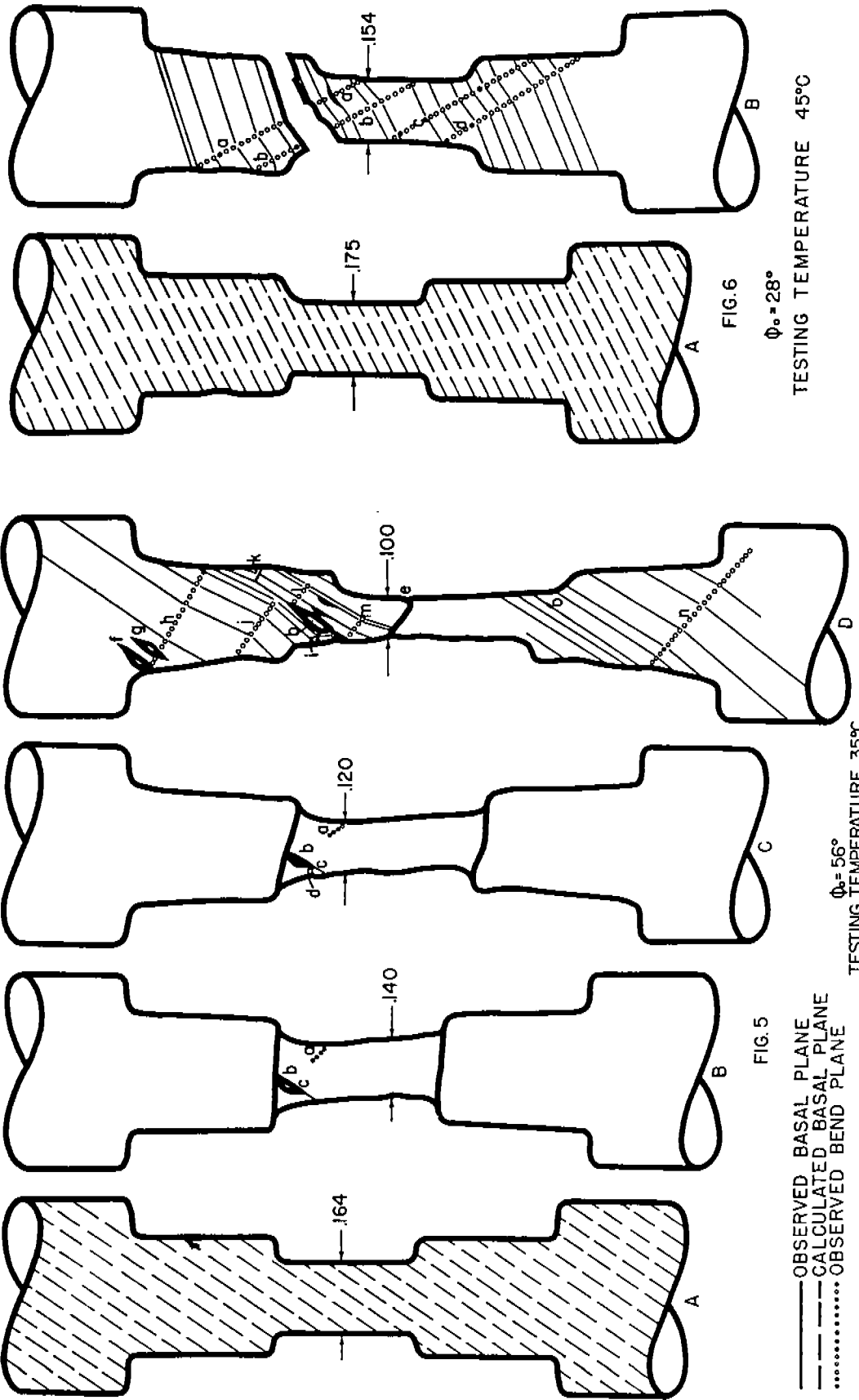
from 0.180 to 0.141 in. The bend-plane (c) was directly observed in part, as shown by circles, and then extrapolated, as shown by the dots. The lower half of the specimen was offset from the upper in respect to the longitudinal axis.

In stage c (Fig. 4c), a crack (g) appeared in the upper shoulder of the specimen. One slip line (d), a projection of the crack, was directly visible, as was the bend-plane (e). Another slip line (f) was drawn parallel to the crack (g), and still another (b) was calculated in a manner similar to that used for the slip lines in stage b.

The section of the specimen immediately below the bend-plane (e) rotated and slipped, causing the observed bend-plane (e) to pivot toward the slip line (d) during the next stage (Fig. 4d). It was thought that while pivoting, the slip line (f) bent into two segments (h and i). These were obtained by drawing lines parallel to the bottom face of the crack (g) and were divided by the bend-plane (j), constructed from the discontinuity in the lower face of the crack (g) to bisect the angle made by the two segments of the slip line (h and i). The bend-plane (c) disappeared from view; this was consistent with the lessening of supposed angular difference between the slip planes (b and i). As a result of these occurrences, the shoulder of the specimen protruded at (k). A lip (l) was produced where the shoulder meets the lower face of the crack (g); this is denoted by the shading in Fig. 4d.

As the processes of stage d continued into stage e, the slip line was observed to swing upward and thus indicated deformation and rotation in the shoulder above the crack. Another slip line appeared (m), parallel to the one already visible (d). The upper face (n) of the crack (g) bent and the shoulder peeled back (o). Two more cracks appeared (p and q).

While stages d and e were maintained, the next stage began (Fig. 4f) with a crack (p) extending toward the surface and propagating a slip line (r) together with a small bend-plane (s). A smaller crack (q) developed a tiny bend-plane (t), and a small crack (u) appeared in the lower head.



In the final stage (Fig. 4g), further deformation produced twinning (v) and secondary cleavage on the basal plane (w) of the twinned metal. The specimen was cooled in liquid nitrogen and cleaved with a razor blade. Using the technique described earlier, the basal planes were traced on the final shadowgraph. These revealed the bend-planes (x, y and z) meeting the crack (p) at points of discontinuity. One bend-plane (aa) accounted for the bend (n) in the upper faces of the crack (g). Bend-planes (aa and z) permitted the shoulder (o) to peel back, while the lip (cc) on the lower face of the crack (p) was formed in a manner similar to the other lip (l). Bend-planes (dd, ee, and ff) appeared in the lower shoulder. The total reduction in area was 54 per cent, and the original crack (g) never grew in length after it had been formed.

#### Case History II (Fig. 5)

In stage a, this crystal had virtually the same initial orientation,  $\theta_0 = 56^\circ$ , as the crystal of Fig. 4, but it was tested at 35 C instead of at 45 C. In Fig. 2, it is located at (b).

In the second stage (Fig. 5b), as the specimen was pulled, a bend-plane (a) became partly visible on the surface. A small crack (b) appeared as did the slip line (c), which was a continuation of the crack. Slip planes were not calculated from the change in diameter, because no bend-plane was observed by which the lower boundary of the slipped material could be constructed.

During the next stage (Fig. 5c), the crack (b) increased in size and sharpness of outline. A bend-plane (d) was observed. The metal immediately above (d) had rotated counterclockwise, so that the basal planes were almost vertical, as shown by the lower left side of the crack (b).

The crystal twinned and failed by secondary cleavage (e) in stage d. New cracks (f and g) appeared in the unslipped portion of the upper shoulder and terminated at the bend-plane (h). A small crack (o) was visible in the lower test section near the shoulder. A bend-plane (i) starting at crack (b) was visible.

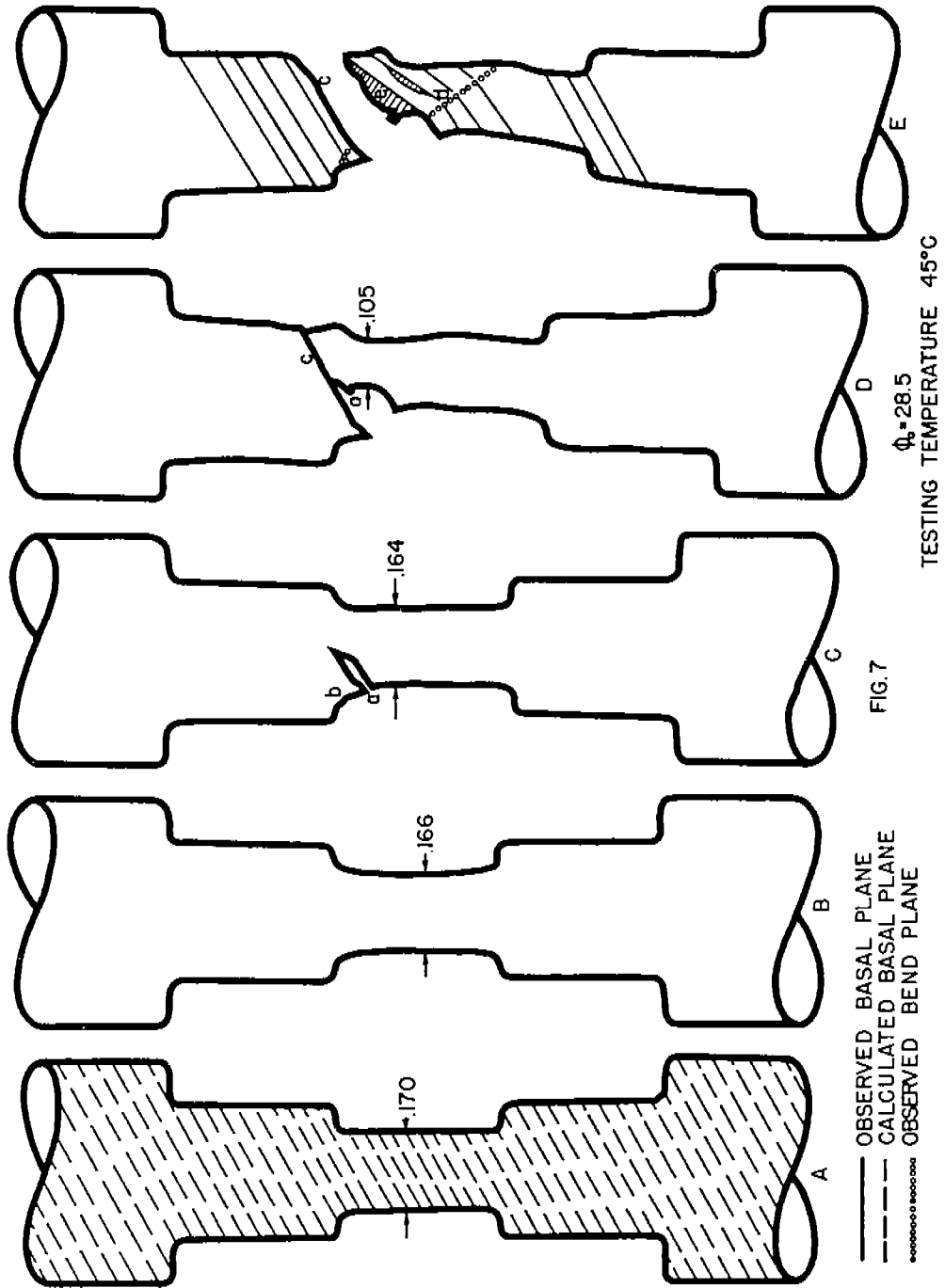
Sectioning of the specimen revealed numerous slip and bend-planes (j--n). Lips (as shown by the shading) also appeared upon sectioning.

Case History III (Figs. 6 and 7)

The crystals in Figs. 6 and 7 were similar in orientation and tested at the same temperature. In stage a, the starting orientation  $\phi_0$ , of the crystal depicted in Fig. 6 was  $28^\circ$  and that of the crystal depicted in Fig. 7 was  $28.5^\circ$ . Their testing temperature was  $45\text{ C}$ , and they are plotted at c in Fig. 2.

The specimen of Fig. 6 was tested in tension during stage b until fracture by primary cleavage occurred. The sections above the bend-plane (a) and below (d) were undeformed, but the sections between (a) and (b) and between (c) and (d) rotated considerably by primary slip. The section between (b) and (c) rotated relatively little. Thus regions of slip alternated with regions of little deformation to permit the elongation of the crystal. This is a manifestation of Andrade and Roscoe's<sup>4</sup> "geometric softening," which has been experimentally observed before in zinc,<sup>5</sup> and is to be expected in tensile tests on crystals having low values of  $\phi$ .

The specimen of Fig. 7 evidenced very little deformation at stage b. The slip planes were not calculated because bend-planes were not observed. A large crack (a) as well as a minute crack (b) above the larger crack appeared near the shoulder of the specimen during the next stage (Fig. 7c). As deformation continued through stage d, the crack (a) opened further and a slip line (c) appeared along the same basal plane as the crack (a). The rotation of the portion of the crystal just below the slip line (c) opened the crack wider and permitted the specimen to elongate. The rotated area is shown by sectioning in stage e. In this stage, little additional tension was required to cause the crack (a) to extend across the crystal. As the crack (a) spread, the surface near the crack held together and deformed before finally severing. The deformed portion (e) was in the form of a lip and gave a cup-shaped appearance to the fracture surface of the lower crystal segment. Sectioning revealed that this deformation extended into the crystal a short distance as shown by the lip (e).



The crystals of Figs. 6 and 7 show in more detail that twinning is not the cause of brittle fracture, because these crystals failed in a brittle manner when twinning did not even occur. In each crystal described, rotation by primary slip produced orientation gradients between the slipped and the unslipped regions. If the orientation gradients could not be accommodated by kink planes or by kink planes and partial cracks, then the crystal would undergo brittle fracture by primary cleavage. On the other hand, if the constraints were accommodated to permit sufficient rotation of the basal planes, then twinning would occur at about  $\theta_f = 80^\circ$ . The twins introduce constraints between the untwinned and twinned metal. These new constraints must be accommodated or brittle fracture will result. By this reasoning, it is seen that what occurs in the twinned section is merely a small scale repetition of what occurs in the crystal as a whole. Twinning introduces no new process but merely introduces constraints.

Morton and Baldwin<sup>1</sup> suggested that if primary cleavage were eliminated by some means such as rotating test grips, Surfaces A, D, and E of Fig. 2 would be extended as shown in Fig. 8. Two approaches were attempted to achieve this. In the first method, specimen grips employing gimbal rings (Fig. 9) were used to permit rotation of the specimen heads in a manner similar to that proposed by Rosi.<sup>6</sup> When the gimbal grips had rotated approximately  $70^\circ$ , the sides of the center section pressed against the specimen and restricted the free rotation of the specimen heads. Thus the constraints were not eliminated and primary cleavage still occurred as shown in Fig. 10. These data on the gimbal grip tests fit the curves of Figs. 11 and 12 for the 0.090-in. dia.,  $A_{\text{shoulder}}/A_{\text{test section}} = 11.1$  specimens. Because of practical difficulties, including the fact that the specimens binded against the grips after limited rotation, this method was discontinued.

The second approach involved limiting the ability of a primary cleavage crack to extend into the specimen shoulder. In Figs. 6 and 7, primary cleavage began in the test section near the shoulder and extended through it. It was rea-

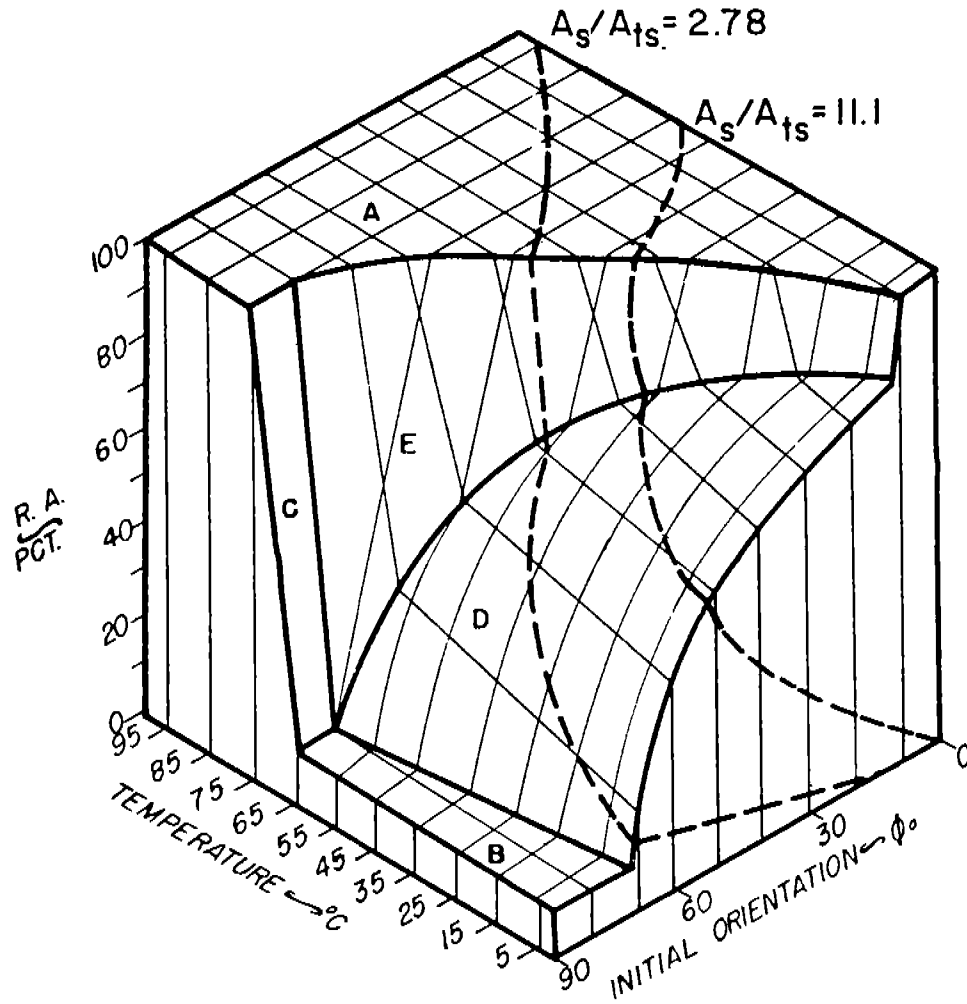


FIG. 8: SUGGESTED COURSE TO FIG. 2 IN THE ABSENCE OF PRIMARY CLEAVAGE INDUCED BY CONSTRAINT OF SHOULDERS OR GRIPS.

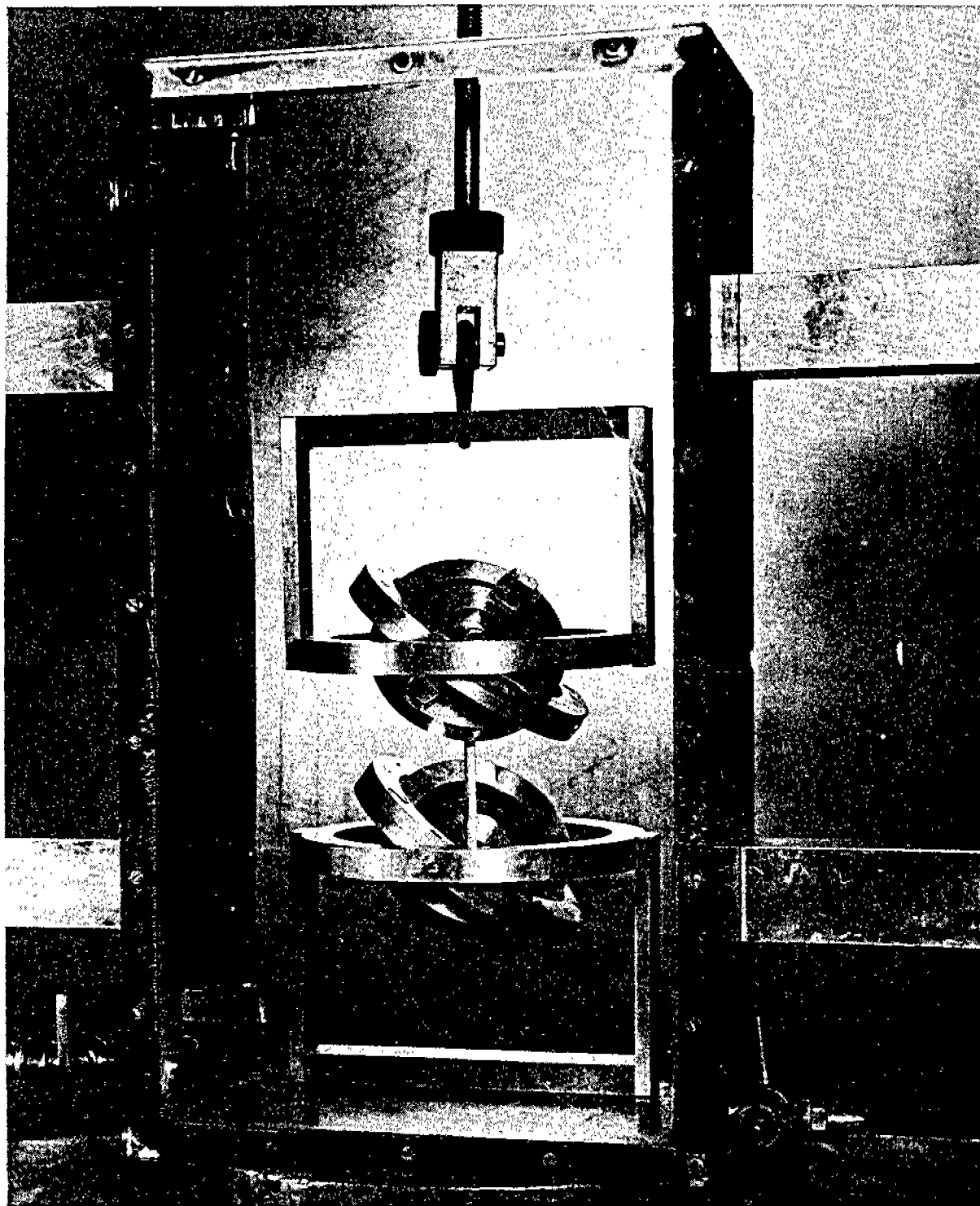


FIG. 9: TEMPERATURE CONTROL BATH SHOWING GIMBAL GRIPS AND TESTED SPECIMEN.

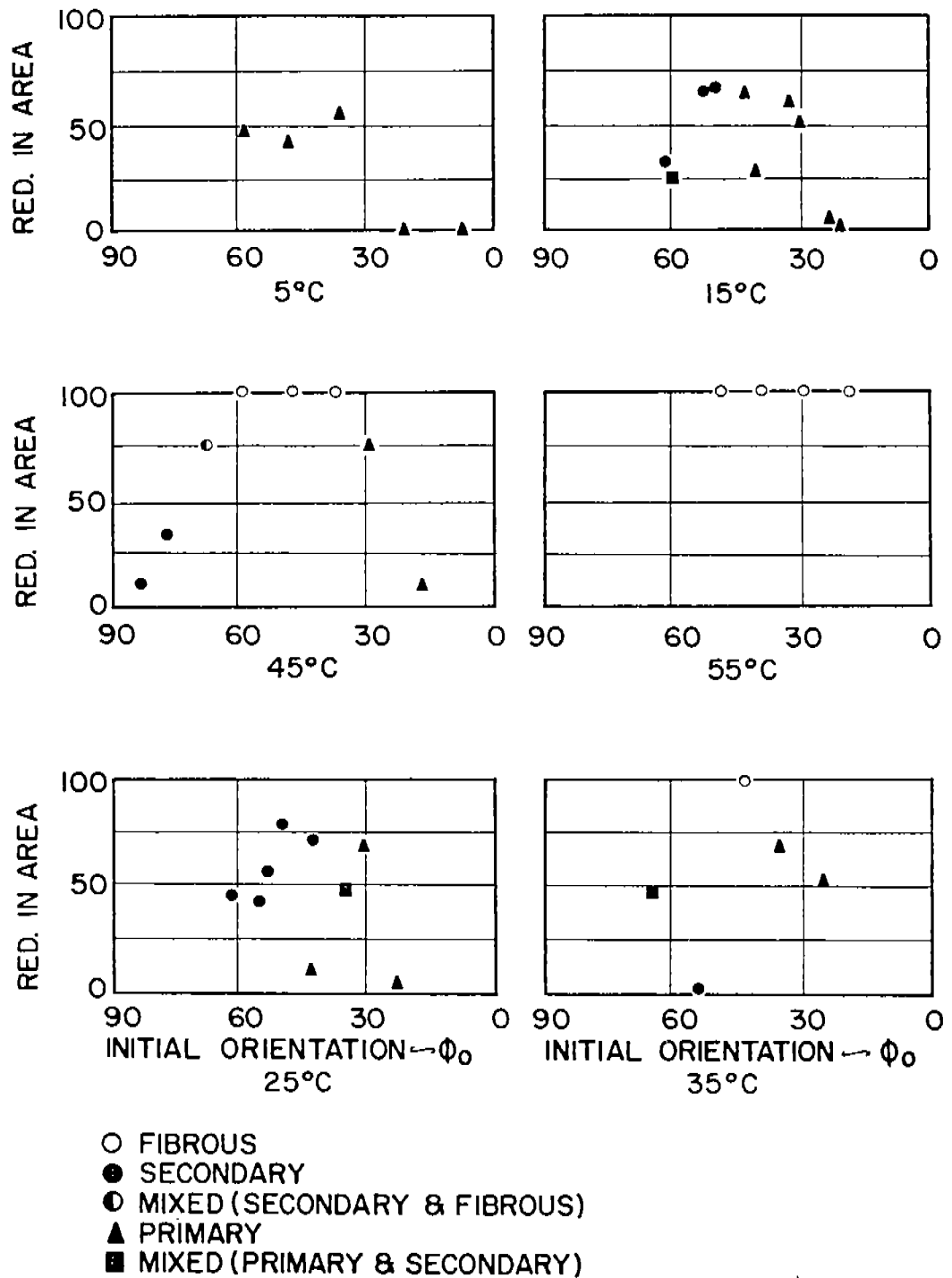


FIG. 10: DUCTILITY (REDUCTION IN AREA) AS A FUNCTION OF INITIAL ORIENTATION,  $\phi_0$ , AT THE TEMPERATURES INDICATED FOR 5D,  $A_S/A_{TS} = 11.1$ , 0.090 IN. DIA. SPECIMENS TESTED WITH THE GIMBAL GRIPS.

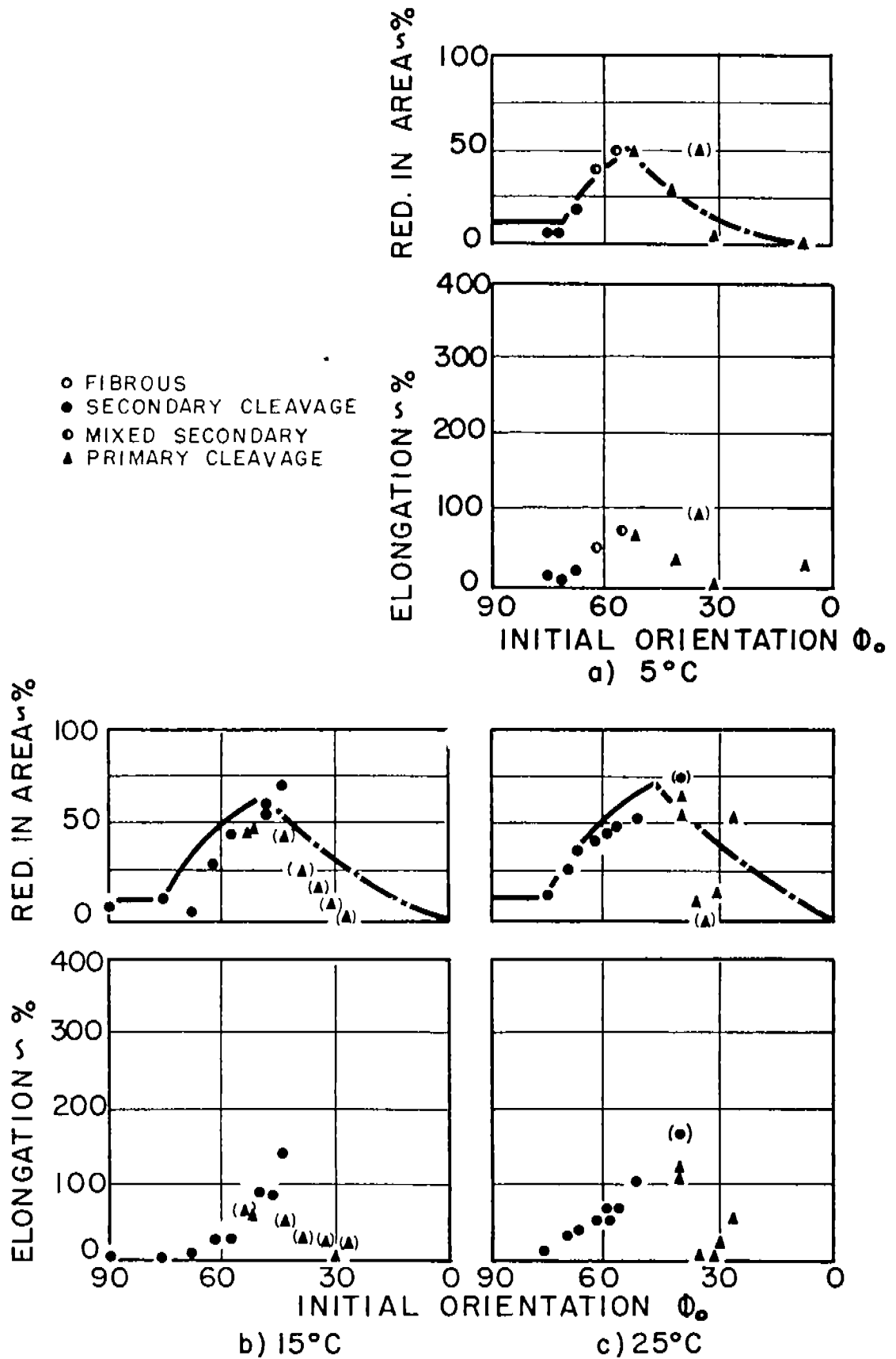


FIG. 11: DUCTILITY (REDUCTION IN AREA AND ELONGATION) AS A FUNCTION OF INITIAL ORIENTATION,  $\phi_0$ , AT THE TEMPERATURES INDICATED FOR 5D,  $A/A_{TS} = 11.1$ , 0.090 IN. DIA. SPECIMENS. (o) INDICATE CRYSTALS WITH SLIGHT ASTERISM OF LAUE SPOTS.

soned that, if the shoulder size were increased relative to that of the test section, the stress in the shoulder and possibly the chance that the crack would penetrate the shoulder would be lowered. This reasoning was based on the fact that the normal stress, acting to pull apart the basal planes to form a crack, varies inversely with the area of cross section under the same applied load. Inasmuch as the cross-sectional area ( $A_s$ ) of the shoulder was 2.78 times that of the cross-sectional area ( $A_{T.S.}$ ) of the test section (Fig. 3), halving the diameter of the test section (Fig. 3b) would give an area ratio of 11.1. In other words, the stress available to continue primary cleavage in the shoulder would be only one-fourth that of the preceding series of specimens. Therefore, a crack started in the test section would be less likely to continue into the shoulder. This allaying of primary cleavage should give increased ductility.

In order to achieve the increase in ductility suggested above, tests were made on crystals with a smaller test section diameter but with the same shoulder diameter (dia. = 0.090 in.,  $A_s/A_{T.S.} = 11.1$ ,  $L/D = 5$ ). Elongation and contraction in area are plotted in Figs. 11--13 as a function of the initial orientation for such specimens. The solid lines show the ideal ductilities as computed by Eq. (1) inserting

$$\cos \phi_f = \frac{\cos \phi_0}{1 + \delta} \quad (2)$$

as given by Schmid and Boas<sup>7</sup> where  $\delta$  is the elongation value. The dot-dash lines represent primary cleavage. The transition zone where fracture may be either ductile or brittle is represented by a shaded area in Fig. 12. Reduction in area values may fall anywhere in this zone. Because the supply of low orientation crystals was limited, some crystals exhibiting asterism in the Laue spots were used to complete the curves. The values from these crystals are enclosed in parentheses in the graphs.

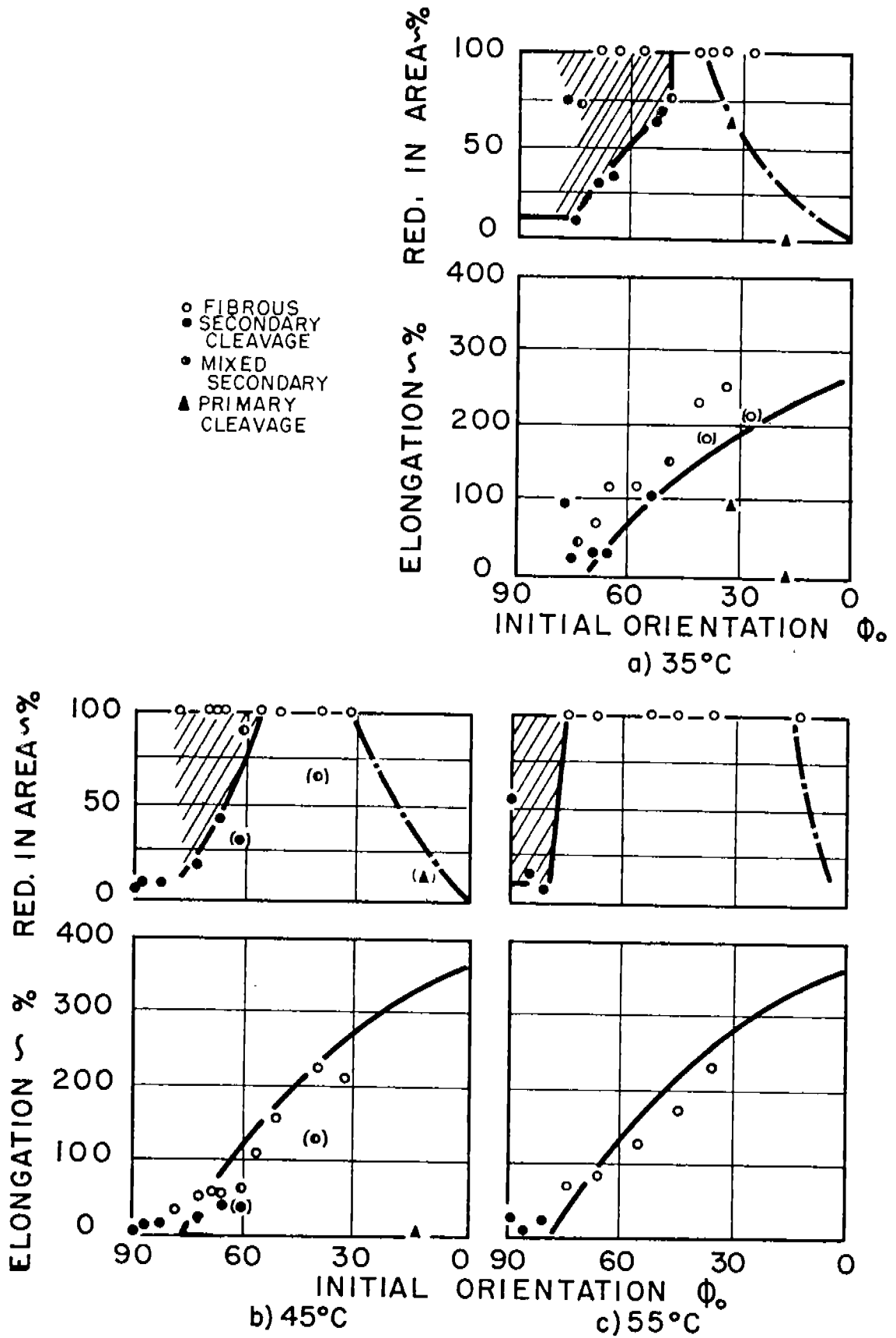


FIG. 12: DUCTILITY (REDUCTION IN AREA AND ELONGATION) AS A FUNCTION OF INITIAL ORIENTATION,  $\phi_0$ , AT THE TEMPERATURES INDICATED FOR 5D,  $A_s/A_{TS} = 11.1$ , 0.090 in. DIA. SPECIMENS. (e) INDICATE CRYSTALS WITH SLIGHT ASTERISM OF LAUE SPOTS.

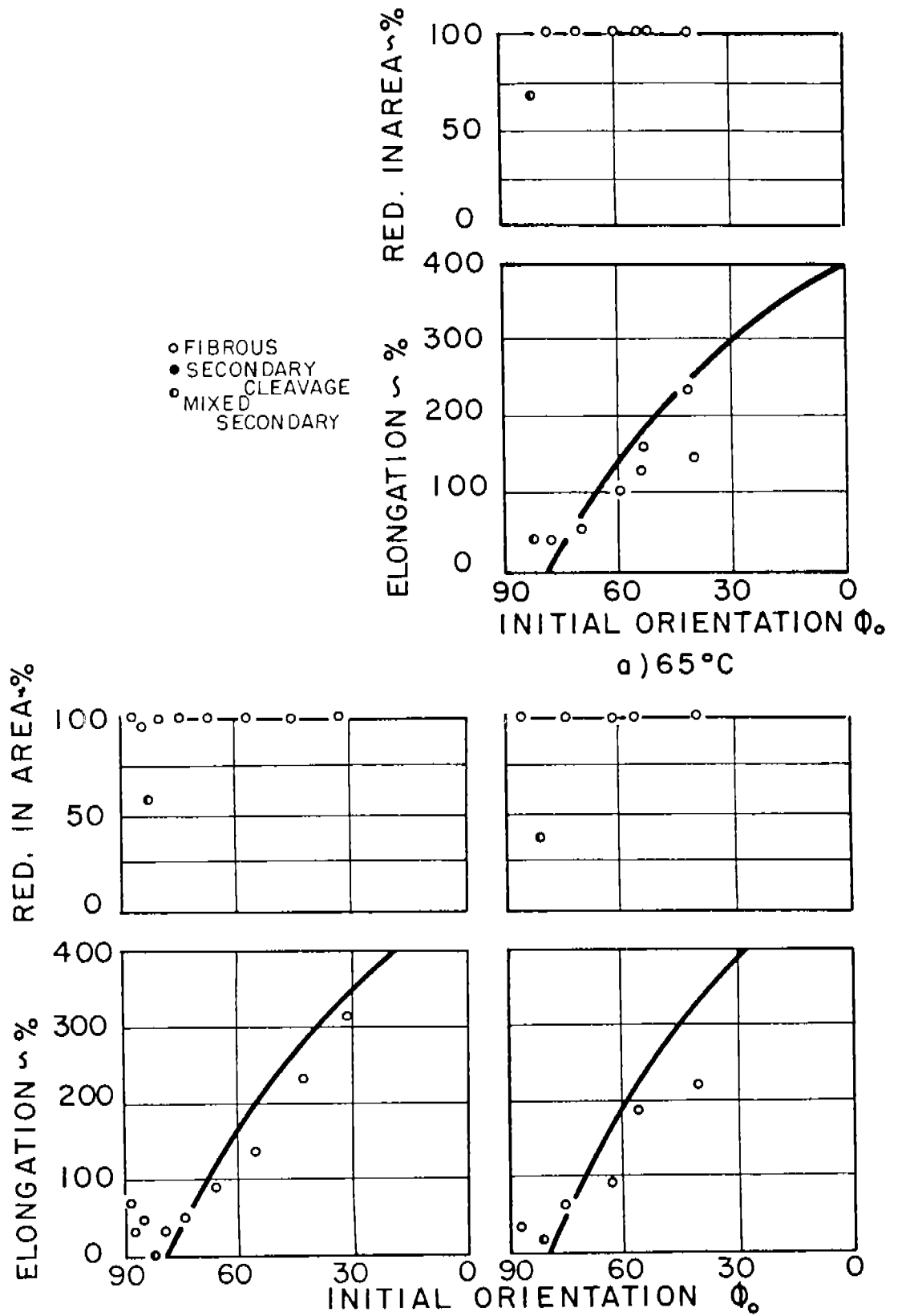


FIG. 13: DUCTILITY (REDUCTION IN AREA AND ELONGATION) AS A FUNCTION OF INITIAL ORIENTATION,  $\phi_0$ , AT THE TEMPERATURES INDICATED FOR 5D,  $A_s/A_{TS} = 11.1, 0.090$  IN. DIA. SPECIMENS.

In Fig. 14, reduction in area is plotted as a function of temperature as derived from data plotted in Figs. 11--13 for all crystals with an initial orientation of  $\phi_0 \geq 80^\circ$ . The shaded area is the ductile-to-brittle transition zone and occurs at the same temperature range as that found by Morton and Baldwin<sup>1</sup> for their 5D,  $A_s/A_{T.S.} = 2.78$  ratio.

Fig. 15 compares reduction in area as a function of orientation of the 5D,  $A_s/A_{T.S.} = 11.1$  ratio with the values obtained by Morton and Baldwin<sup>1</sup> for their 5D,  $A_s/A_{T.S.} = 2.78$  ratio. Reduction in area values for both series when  $\phi_0 = 80^\circ$  corresponded closely, as would be expected from the preceding paragraph. In both series, crystals of  $\phi_0 = 70^\circ$  rotated by primary slip, twinned, and fractured by secondary cleavage to the same extent when tested at 5 C; at  $\phi_0 = 65^\circ$ , however, the  $A_s/A_{T.S.} = 2.78$  specimens failed by primary cleavage, while those with  $A_s/A_{T.S.} = 11.1$  twinned, failed by secondary cleavage, and showed greater ductility. At  $\phi_0 = 67^\circ$ , Morton and Baldwin's crystals reached a ductility maximum of 18 per cent, but those of this report attained a maximum ductility of 50 per cent when  $\phi_0 = 55^\circ$ . Thus the larger ratio of shoulder to test section area lessened the primary cleavage range and increased the ductility over a large initial orientation range. Similar behavior is seen in the results of tests at temperatures of 35, 45, and 55 C. Tests at high temperatures and low orientations would have been desirable, but the supply of such crystals ran out.

In extending Surfaces A, D, and E (Fig. 8) by allaying primary cleavage, i. e. changing the conditions of constraint to permit more primary slip, it was demonstrated dramatically that twinning itself is not a cause of brittle fracture, but that the orientation gradients set up by the constraints determine the type of fracture. The dotted line to the left (for  $A_s/A_{T.S.} = 2.78$ ) represents the intersection of this suggested figure with the primary cleavage face (F) of Fig. 2. The dotted line to the right ( $A_s/A_{T.S.} = 11.1$ ) shows the intersection of the primary cleavage face of the present data as plotted in Figs. 11--13. Surface E was lowered about

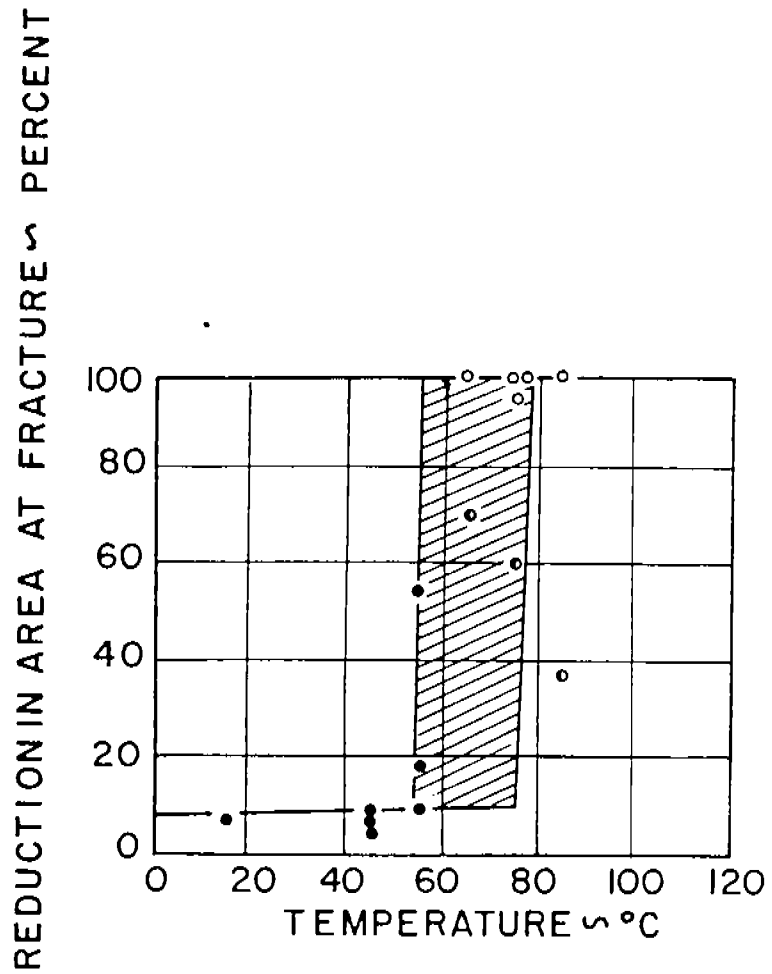


FIG. 14: REDUCTION IN AREA AS A FUNCTION OF TEMPERATURE FOR SPECIMENS WITH INITIAL ORIENTATION  $\approx 80^\circ$ . THESE GRAPHS ARE CROSS PLOTS OF THE DATA (FOR SPECIMENS  $\approx 80^\circ$ ) GIVEN IN FIGS. 10, 11 and 12.

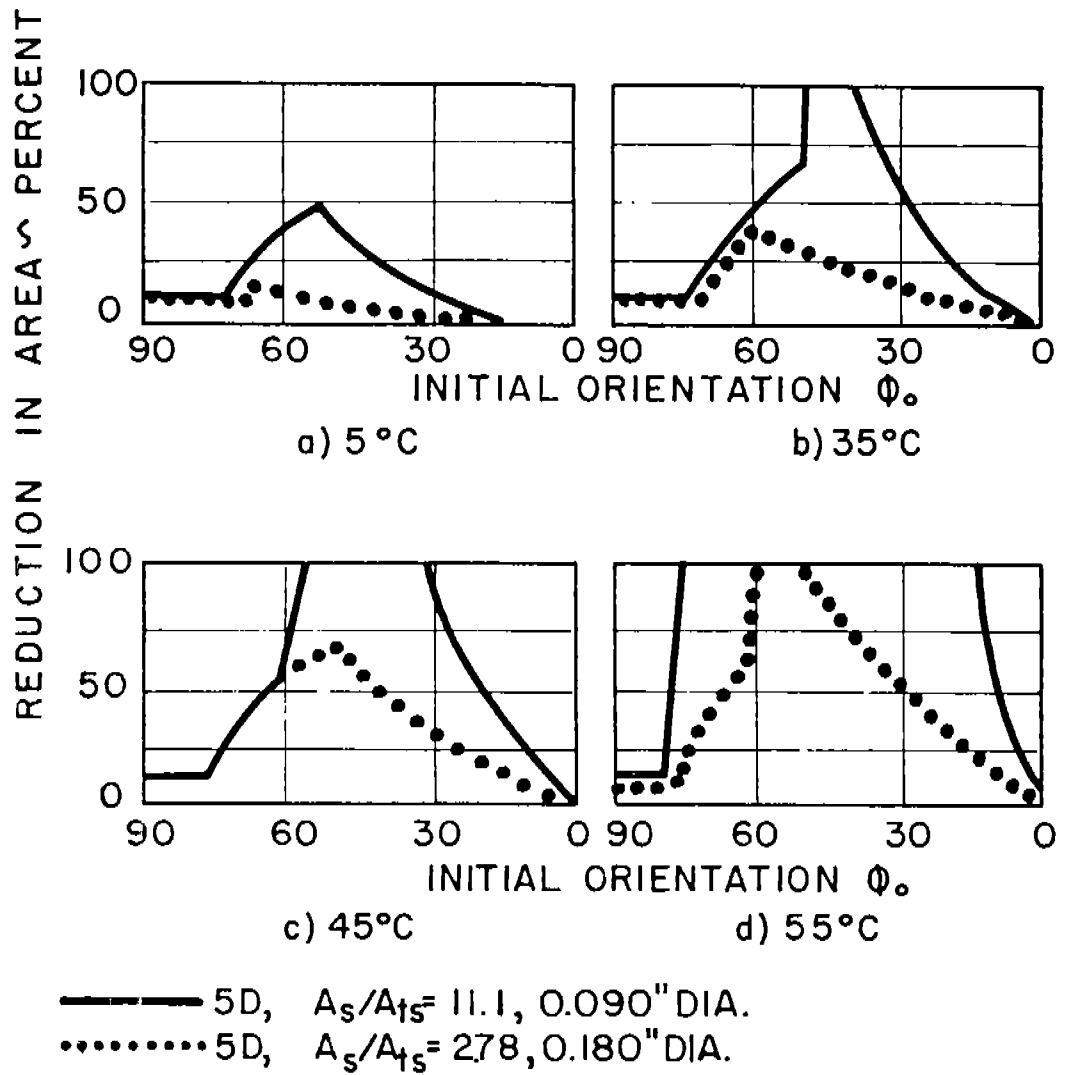


FIG. 15: DUCTILITY (REDUCTION IN AREA) AS A FUNCTION OF INITIAL ORIENTATION,  $\phi_0$ , AT TEMPERATURES FOR WHICH SUFFICIENT DATA WERE AVAILABLE FOR COMPARISON.

10 C in temperature for the  $A_s/A_{T.S.} = 11.1$  specimens, but this is within experimental error and can be ignored in the idealized drawing. At the same testing temperature (e.g. 5 C), two crystals of identical orientation ( $\theta_0 = 55^\circ$ ) but different constraints (in this case,  $A_s/A_{T.S.} = 11.1$  and 2.78 respectively) could have widely different degrees of ductility. The first crystal would slip, twin and cleave secondarily and show greater ductility than the second crystal which did not twin but cleaved.

The higher ductility of the  $A_s/A_{T.S.} = 11.1$  specimens as compared with those of  $A_s/A_{T.S.} = 2.78$  appeared to be caused by the increased  $A_s/A_{T.S.}$  ratio but might have been due to the size effect of the different test section diameters. To check this, tests were started on crystals of double the head and shoulder diameters with  $A_s/A_{T.S.}$  ratios of 2.78 and 11.1. Table I is a summary of test specimen dimensions.

TABLE I SPECIMEN DIMENSIONS

Test Section Diameter, in.	Shoulder Diameter, in.	<u>Area of Shoulder</u> <u>Area of Test Section</u> ( $A_s/A_{T.S.}$ )	Test Section Length, in.	<u>Test Section Length</u> <u>Test Section Diameter</u>
.180	.300	2.78	.180	1 D
.180	.300	2.78	.360	2 D
.180	.300	2.78	.900	5 D
.090	.300	11.1	.450	5 D
.360	.600	2.78	1.800	5 D
.180	.600	11.1	.900	5 D

Fig. 16 shows the results of the tensile tests on specimens .360 in. in diameter with  $A_s/A_{T.S.} = 2.78$ , (that is, double the size but of the same proportions as the

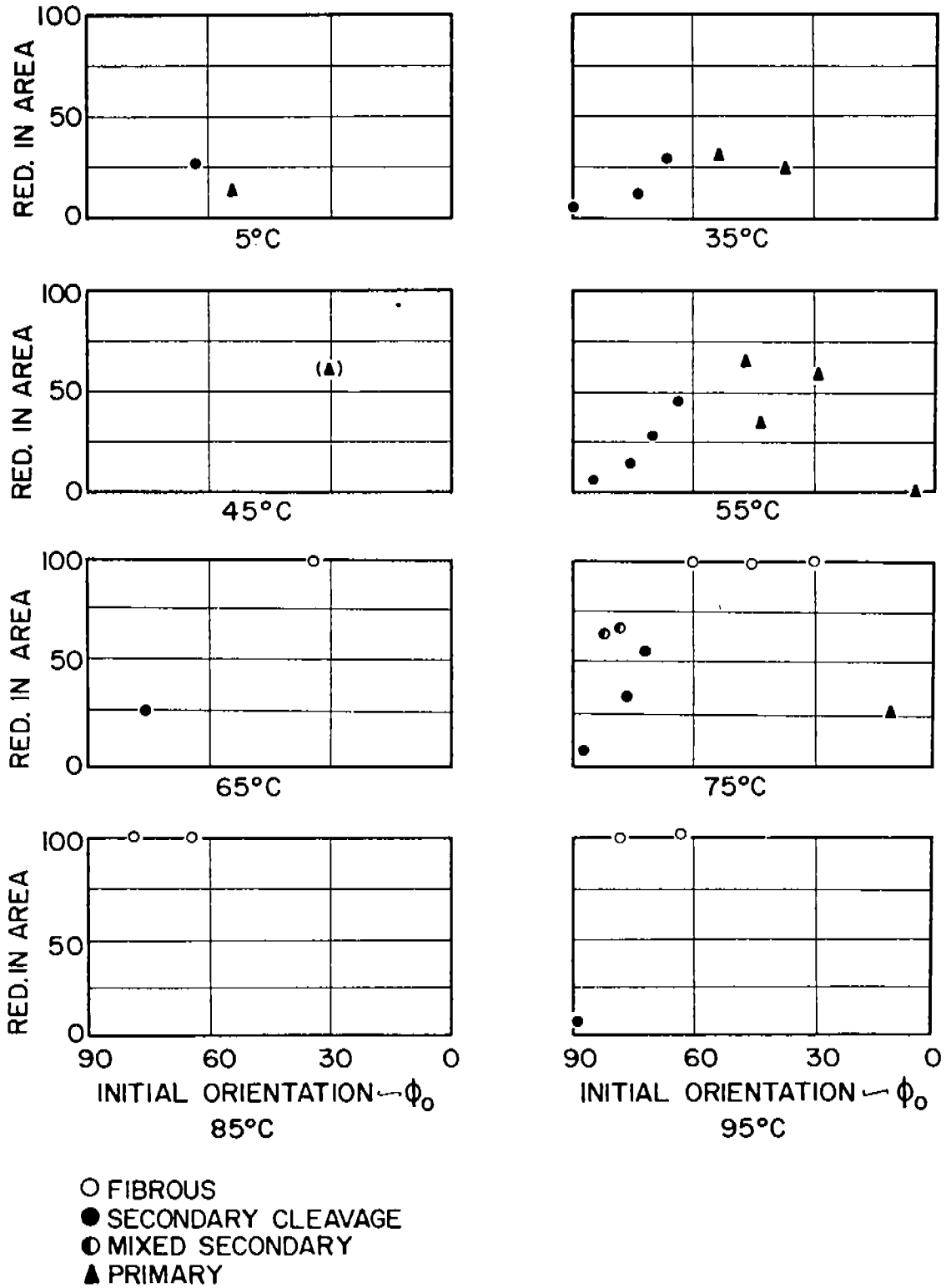


FIG. 16: DUCTILITY (REDUCTION IN AREA) AS A FUNCTION OF INITIAL ORIENTATION,  $\phi_0$ , AT THE TEMPERATURES INDICATED FOR 5D, 0.360 IN. DIA.,  $A_s/A_{TS} = 2.78$  SPECIMENS.

specimens in Fig. 3a). These data coincide with those obtained in the previous report.<sup>1</sup> The ductility (reduction in area) at fracture as a function of initial orientation and temperature is plotted in Fig. 17 for all  $A_s/A_{T.S.} = 2.78$  crystals that broke by primary cleavage. Although further data are really needed here, it can still be seen that the size differences did not noticeably affect the fractures by primary cleavage, inasmuch as the data for the two sizes coincide.

The paucity of points in Fig. 18 for specimens .180 in. in diameter with  $A_s/A_{T.S.} = 11.1$  (twice the size of those in Fig. 3b) is caused by difficulties in successfully growing single crystals of this size and shape in the desired orientations. Further tests should be made for the results to be conclusive, but the few results obtained do fit the data of the smaller sized but similarly shaped specimens shown in Figs. 11 and 12.

#### IV. CONCLUSIONS

Kinematic studies show directly that primary cleavage occurs on the basal planes on the non-slipping or inert side of a bend-plane. In the specimens used here, the bend-planes are close to the shoulder and the cleavage runs from the bend-plane into the shoulder itself.

There the cleavage crack may 1) stop, the crystal pivoting about the end of the crack by means of a system of bend-planes until the orientation of the test crystal reaches  $\phi_f$ , the critical orientation for twinning, at which point the crystal twins, goes into secondary slip and finally breaks with 100 per cent reduction in area; 2) stop, the crystal behaving as described above up to and including the point of twinning, after which it cleaves by secondary cleavage; or 3) continue across the shoulder ending in a complete fracture by primary cleavage.

Increasing the size of the shoulder relative to the area of the actively slipping test section represses the third alternative and favors the first two, indicating that propagation of the crack through the shoulder depends upon the magni-

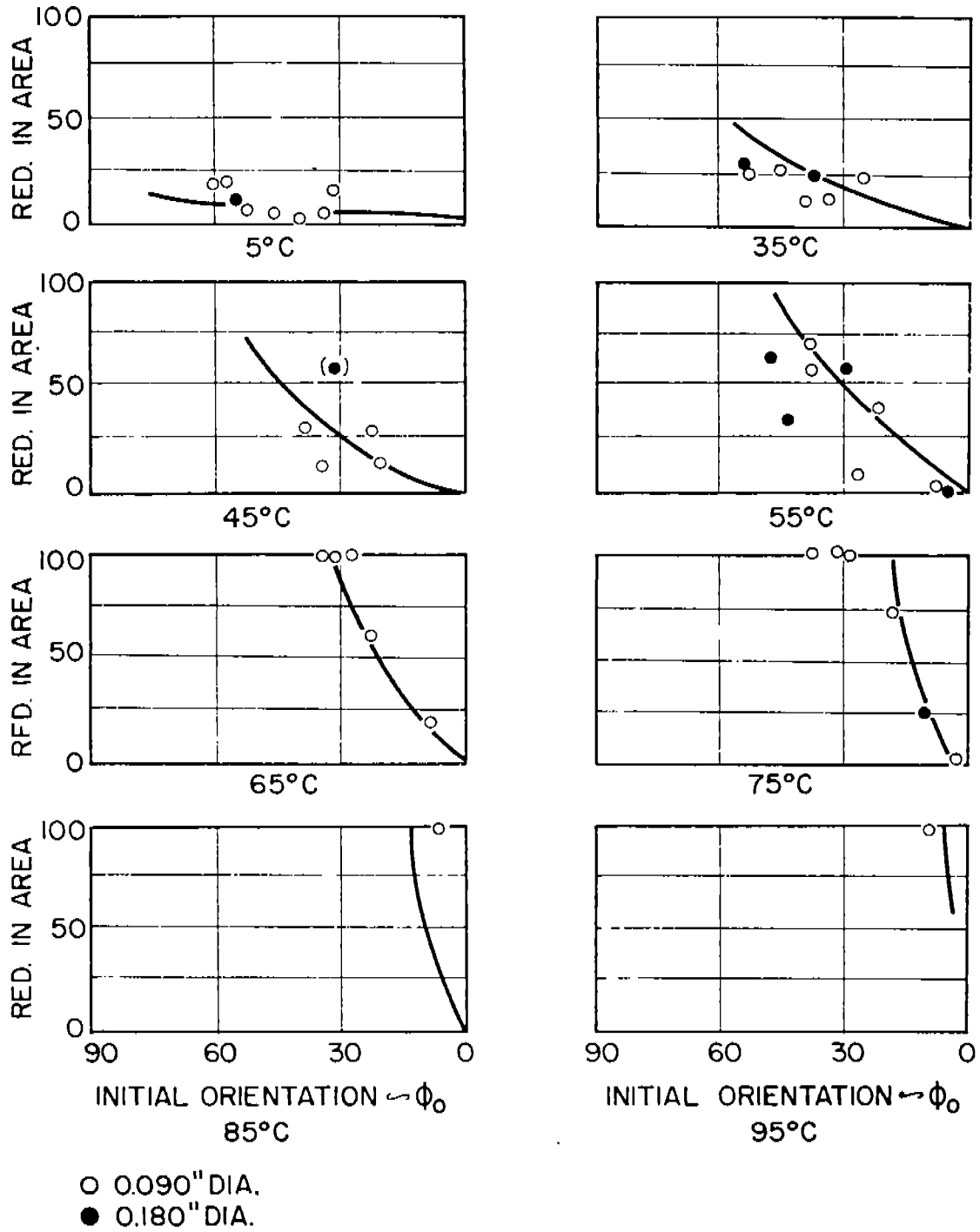


FIG. 17: DUCTILITY (REDUCTION IN AREA AT FRACTURE) AS A FUNCTION OF INITIAL ORIENTATION,  $\phi_0$ , for  $A_s/A_{TS} = 2.78$  SPECIMENS WHICH BROKE BY PRIMARY CLEAVAGE.

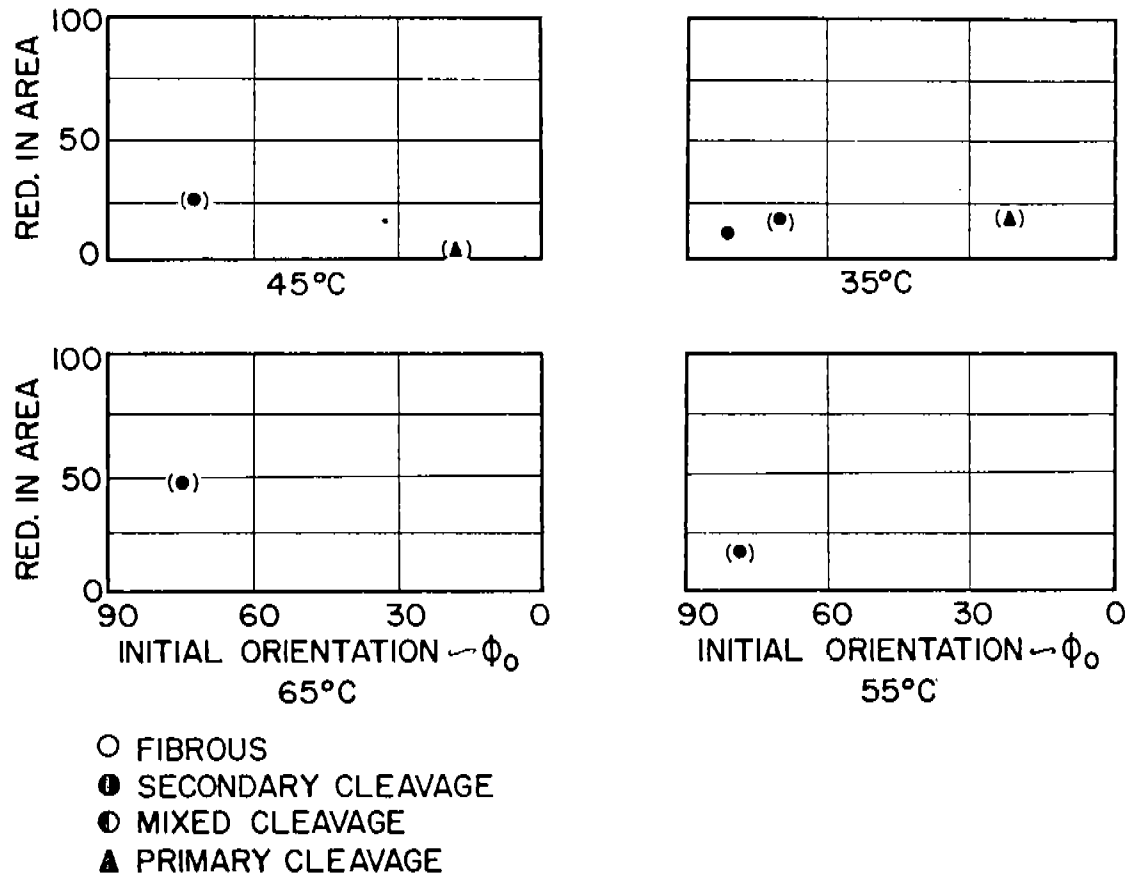


FIG. 18: DUCTILITY (REDUCTION IN AREA) AS A FUNCTION OF INITIAL ORIENTATION,  $\phi_0$ , AT THE TEMPERATURES INDICATED FOR 5D, 0.180 IN. DIA.,  $A_s/A_{TS} = 11.1$  SPECIMENS. (\*) INDICATE ASTERISM OF LAUE SPOTS.

tude of stress there. This probably represents a geometric rather than a size effect, since a few tests made on geometrically similar samples of different sizes produced the same results.

The inability of bend-planes to accommodate orientation gradients in zinc when low temperature promotes the appearance of primary cleavage is of enormous importance, for it at once gives a clue to why secondary cleavage appears. Secondary and primary cleavage both occur on the basal plane, and they both occur in regions adjacent to orientation gradients: primary cleavage in the shoulder, where slip is restricted to the broader portion of the crystal, and secondary cleavage in a twin band, where orientation gradients must develop adjacent to the twin boundaries to maintain compatibility.<sup>8</sup> It is proposed, therefore, that secondary cleavage is fundamentally the same as primary cleavage, differing only in the manner in which the orientation gradient that induces basal cleavage is developed.

The inability of bend-planes to accommodate orientation gradients as temperature is lowered is of importance, too, in the case of polycrystalline specimens. Here, orientation gradients are as numerous as the grains of the sample at hand, since they are a common mode by which compatibility between the grains is effected.<sup>9--16</sup> If the gradients can not be accommodated by kinking, cleavage may be expected to result. It is to be expected that the conditions for cleavage in different grains will be reached at different stages in a polycrystalline aggregate. Homes and Gouzou<sup>17</sup> have shown by direct observation of the process of fracture that this is the case for zinc when it is below the transition temperature. It was not until a large number of "premature" cracks had formed that rapid cleavage cut through the remaining grains.

In order to discover the mechanism of low temperature embrittlement, the mechanical behavior of single crystals must be more completely described and understood. The work of this project has disclosed a number of interesting phe-

nomena worthy of further investigation. An examination of the process of fracture of a typical crystal presents some new questions. Cracks form, extend into the crystal and stop; the remaining section of the crystal then rotates, elongates, and withstands a greater stress than the original uncracked section. Why should this mysterious sequence of events often occur? What factors govern the amount of rotation prior to the appearance of the first crack? Is the amount of rotation constant? How much rotation occurs following the initial crack? What effect does the manner of fracture have upon the degree of rotation? All of these questions are of basic interest in the study of the mechanism of low temperature embrittlement.

Using the same test section but varying the head size caused ductility changes. The roles that orientation gradients and the stresses from orientation gradients play should be studied in detail. Why rotation of the bend-planes should cease below certain temperatures and what causes its orientation independence are questions of utmost importance yet to be answered.

## V. REFERENCES

1. Morton, P. H., and Baldwin, W. M., Jr., Low Temperature Embrittlement Mechanics Deduced from Zinc Single Crystal Fracture Studies (Ship Structure Committee Report Serial No. SSC-58), Washington: National Academy of Sciences-National Research Council, May 1, 1953.
2. Mark, H., Polanyi, M., and Schmid, E., "Processes in the Straining of Zinc Crystals," Zeitschrift für Physik, vol. 12, pp. 58-116 (1923).
3. Mathewson, C. H., and Phillips, A. J., Plastic Deformation of Coarse-Grained Zinc (AIME Trans. No. 1623-E), New York: American Institute of Mining and Metallurgical Engineers, January 1927.
4. Andrade, E. N. daC., and Roscoe, R., "Glide in Metal Single Crystals," Proc., Phy. Soc., vol. 49, p. 152 (1937).
5. Cottrell, A. H., and Aytakin, V., "The Flow of Zinc under Constant Stress," J. Inst. of Metals, vol. 77, p. 389 (1950).
6. Rosi, F. D., "Homogeneous Extension of Single Crystals," Review of Scientific Instruments, 22:9, p. 708 (September 1951).
7. Schmid, E., and Boas, W., Kristallplastizität mit besonder Berücksichtigung der Metalle, Berlin: Julius Springer. (Translation: Plasticity of Crystals with Special Reference to Metals, London: F. A. Hughes and Company, Ltd., 1950.)
8. Pratt, P. L., and Pugh, S. F., "Twin Accommodation in Zinc," J. Inst. of Metals, vol. 80, pp. 653-658 (August 1952).
9. Kawada, T., "The Plastic Deformation of Zinc Bicrystals," Proc. First World Metallurgical Congress ASM, pp. 591-602 (1951).
10. Barrett, C. S., and Levenson, L. H., "The Structure of Aluminum after Compression," Trans., Inst. of Metals Division, AIME, vol. 137, pp. 112-126 (1940).
11. Woodard, D. H., "Stages in the Deformation of Monel Metal as Shown by Polarized Light," Trans., Metals Branch, AIME, vol. 185, pp. 722-726 (October 1949).
12. Honeycombe, R. W. K., "Inhomogeneity of Deformation in Metal Single Crystals," Proc., Phy. Soc., vol. 63A, pp. 672-673 (1950).

13. Laurent, R., and Eudier, M., "Crystalline Interaction and the Brittleness of Metals," Revue de Metallurgie, vol. 47, pp. 582-587 (August 1950).
14. King, R., and Chalmers, B., "Crystal Boundaries," Progress in Metal Physics (1), pp. 127-162, New York: Interscience Publishers, Inc., 1949.
15. Chalmers, B., "The Influence of Difference of Orientation of Two Crystals on the Mechanical Effect of Their Boundary," Proc., Royal Society, vol. A162, pp. 120-127 (1937).
16. Washburn, J., and Parker, E. R., "Kinking in Zinc Single Crystal Tension Specimens," Trans., AIME, vol. 194, pp. 1076-1078 (1952).
17. Homes, G. A., and Gouzou, J., "A Study of the Mechanism of Fracture of Metals," Revue de Metallurgie, vol. 47, pp. 678-692 (September 1950).